

# Transport coefficients for BET

M. M. Basko, ITEP-MPQ, 2002

(Dated: January 28, 2007)

## Contents

<b>1. Target state</b>	1
1.1. Chemical composition	2
1.2. Thermodynamic state	2
<b>2. Stopping power</b>	3
2.1. Bohr-Bethe-Bloch electronic stopping power	3
1. General expression for the electronic stopping power	3
2. Shell corrections	4
3. Mean excitation energies $\hbar\bar{\omega}_{kij}$	5
2.2. Electronic stopping of neutral projectiles	5
1. Stopping on target atoms and ions	5
<b>3. Energy straggling</b>	6
<b>4. Charge change rates</b>	6
<b>5. Cross-sections: projectile <u>ionization</u> in collisions with <u>free electrons</u></b>	7
5.1. <u>Theory-1</u> option: the Lotz formula	7
<b>6. Cross-sections: projectile <u>recombination</u> in collisions with <u>free electrons</u></b>	7
6.1. <u>Theory-1</u> option: a simple and universal theoretical model	7
<b>7. Cross-sections: projectile <u>ionization</u> in collisions with target ions (atoms)</b>	8
7.1. <u>Theory-1</u> option: a universal theoretical model for ionization into continuum	8
7.2. <u>Experiment-1</u> option:	11
1. Ionization of H projectiles in collisions with the H <sub>2</sub> molecules	11
2. Ionization of H projectiles in collisions with the H <sup>+</sup> ions	12
3. Ionization of H projectiles in collisions with the O <sub>2</sub> molecules	13
<b>8. Cross-sections: projectile <u>recombination</u> in collisions with target ions (atoms)</b>	13
8.1. <u>Theory-1</u> option: a universal theoretical model for the electron transfer in collisions between two ions	13
8.2. <u>Theory-2</u> option: Phaneuf <i>et al.</i> formula for the electron transfer	14
1. Recombination of arbitrary ions in collisions with the H <sub>2</sub> molecules, H and He atoms	14
8.3. <u>Experiment-1</u> option:	15
1. Recombination of protons in collisions with the H <sub>2</sub> molecules	15
2. Recombination of protons in collisions with the O <sub>2</sub> molecules	16
<b>9. Initial conditions for the distribution function</b>	16
<b>A. Stopping theory</b>	17
A.1. Interpolation between the Bohr and Bethe Coulomb logarithms	17
<b>B. Model for atomic screening</b>	18
B.1. The limit of $Z \gg 1$	18
B.2. Hydrogen atom and hydrogen-like ions	20
B.3. Ionic radius $r_a$	20
B.4. Momentum transfer to a fast electron	21
<b>References</b>	21

## 1. TARGET STATE

The target state is characterized by its (i) chemical composition, and (ii) thermodynamic state. In general, all the parameters describing the target state may be functions of coordinate  $x$  along the direction of beam propagation.

### 1.1. Chemical composition

We assume that the target material is a compound substance consisting of identical “molecules”. Its chemical composition is characterized by a set of stoichiometric coefficients  $\nu_k$  ( $k = 1, 2, \dots, N_{trgk}$ ), i.e. each “molecule” contains  $\nu_k$  atoms of an element  $k$  with the atomic number  $Z_{tk}$  and atomic mass  $A_{tk}$ . Correspondingly, we introduce a molecular mass as

$$A_{tmol} = \sum_k \nu_k A_{tk}. \quad (1.1.1)$$

The stoichiometric coefficients  $\nu_k$  can have arbitrary normalization because it cancels out in the final formulas.

### 1.2. Thermodynamic state

In thermodynamic equilibrium, the thermodynamic state of the target material is fully defined by the values of the target density  $\rho$ , its electron,  $T_e$ , and ion,  $T_i$ , temperatures. The latter means, that there should exist an algorithm for calculating the detailed set of thermodynamic parameters from given  $\rho$ ,  $T_e$ , and  $T_i$ .

The detailed set of thermodynamic parameters includes the following quantities. First of all, these are the fractional concentrations  $c_{tki}$  of the  $i$ -th ionization stage for each element  $k$ . We assume that the index  $i = 1, 2, \dots, Z_{tk} + 1$  ( $i = 1$  corresponds to the neutral atom), where the degree of ionization is  $y_{tki} = i - 1$ , and  $+ey_{tki}$  is the electric charge of the ion  $i$ . The concentrations  $c_{tki}$  are assumed to be normalized by the condition

$$\sum_{i=1}^{Z_{tk}+1} c_{tki} = 1 \quad (1.2.1)$$

for each  $k$ . The mean ion charge  $\bar{y}_{tk}$  of the element  $k$  is defined as

$$\bar{y}_{tk} = \sum_{i=1}^{Z_{tk}+1} c_{tki} y_{tki} = \sum_{i=2}^{Z_{tk}+1} (i-1) c_{tki}. \quad (1.2.2)$$

Another quantity that should belong to the detailed set of thermodynamic parameters, is the effective number  $\tilde{n}_{kij}$  of the bound electrons in the electronic subshell  $j$  (characterized by the quantum numbers  $nlj$ ) of the ion  $i$  of the element  $k$ . For each ion  $ki$ , the distribution of the given number of bound electrons,

$$\sum_j \tilde{n}_{kij} = Z_{tk} - y_{tki}, \quad (1.2.3)$$

over the electronic subshells will, in general, depend on  $\rho$  and  $T_e$ . As a zero option, we assume that  $\tilde{n}_{kij}$  are equal to the subshell populations of the isolated “cold” atom with removed  $y_{tki}$  outer electrons.

Option 1 (IFTSTAT1=1). In this option all the thermodynamic parameters are assumed to be provided from outside.

Option 2 (IFTSTAT1=2). In this option only the main parameters  $\rho$ ,  $T_e$ , and  $T_i$  are assumed to be provided from outside, whereas the detailed set of parameters is calculated in the internal SAHA routine, which solves the system of the Saha equations for given  $\rho$ ,  $T_e$ , and chemical composition.

The numbers of the free electrons,  $n_{fe}$  [ $\text{cm}^{-3}$ ], of the ions of sort  $ki$ ,  $n_{ki}$  [ $\text{cm}^{-3}$ ], and of the bound electrons in the ions of sort  $ki$ ,  $n_{be,ki}$  [ $\text{cm}^{-3}$ ], per unit volume are given by

$$n_{fe} = \frac{\rho}{A_{tmol} m_u} \sum_k \nu_k \bar{y}_{tk} = \frac{\rho y_{tmol}}{A_{tmol} m_u}, \quad n_{ki} = \frac{\rho}{A_{tmol} m_u} \nu_k c_{tki}, \quad n_{be,ki} = n_{ki} (Z_{tk} - y_{tki}), \quad (1.2.4)$$

where  $m_u = 1.66054 \times 10^{-24}$  g is the atomic mass unit, and

$$y_{tmol} = \sum_k \nu_k \bar{y}_{tk} = \sum_k \nu_k \sum_i (i-1) c_{tki} \quad (1.2.5)$$

is the number of free electrons per “molecule”.

## 2. STOPPING POWER

### 2.1. Bohr-Bethe-Bloch electronic stopping power

#### 1. General expression for the electronic stopping power

We use the following expression for the stopping power on target electrons for a point-charge projectile with the electric charge  $+ey_p$  ( $y_p = 1, 2, \dots$ ), velocity  $v_p$  ( $\beta_p = v_p/c$ ), kinetic energy  $E_p$

$$\begin{aligned} -\frac{dE_p}{dx} &= \frac{4\pi e^4 y_p^2}{m_e v_p^2} \left( n_{fe} G(x_e) L_{fe} + \sum_{k,i,j} n_{ki} \tilde{n}_{kij} L_{be,kij} \right) = \\ &= 0.307075 \frac{y_p^2}{\beta_p^2} \frac{\rho}{A_{tmol}} \left\{ y_{tmol} G(x_e) L_{fe} + \sum_k \nu_k \left[ \sum_i c_{tki} \sum_j \tilde{n}_{kij} L_{be,kij} \right] \right\}. \quad [\text{MeV/cm}] \end{aligned} \quad (2.1.1)$$

Here  $L_{fe}$  is the Coulomb logarithm of the free electrons, and  $L_{be,kij}$  is the Coulomb logarithm of the bound electrons in the subshell  $j$  of the ion  $i$  of the element  $k$ . If not stated to the contrary, the CGS units are used in all ‘‘practical’’ formulas. We make use of the simple Bragg rule (for more details see Ref. [4]) to calculate the stopping power of a compound substance.

In the fully relativistic case we have the following relation between the projectile kinetic energy  $E_p$  and its velocity  $v_p = \beta_p c$ :

$$\gamma_p = 1 + \epsilon_p, \quad \beta_p^2 = \epsilon_p \frac{2 + \epsilon_p}{(1 + \epsilon_p)^2}, \quad (2.1.2)$$

where

$$\epsilon_p = \frac{E_p}{A_p m_u c^2} = 1.07354 \times 10^{-3} \frac{E_{p,MeV}}{A_p}, \quad (2.1.3)$$

$A_p$  and  $Z_p$  are, respectively, the atomic mass and the atomic number of the projectile.

The thermal (or Fermi) motion of the plasma electrons is accounted for by introducing the Chandrasekhar function  $G(x_e)$ ,

$$\begin{aligned} G(x) &= \frac{2}{\sqrt{\pi}} \left( \int_0^x e^{-t^2} dt - x e^{-x^2} \right) = \\ &= \begin{cases} \frac{4}{3\sqrt{\pi}} x^3 e^{-x^2} \left( 1 + \frac{2}{5} x^2 + \frac{4}{35} x^4 + \frac{8}{315} x^6 + \dots \right), & 0 \leq x \leq 0.5, \\ 1 - \left( a_1 t + a_2 t^2 + a_3 t^3 + \frac{2}{\sqrt{\pi}} x \right) e^{-x^2}, & 0.5 < x < +\infty, \\ t = \frac{1}{1 + 0.47047 x}, \quad a_1 = 0.3480242, \quad a_2 = -0.0958798, \quad a_3 = 0.7478556, \end{cases} \end{aligned} \quad (2.1.4)$$

in front of  $L_{fe}$ , where

$$x_e = \left( \frac{m_e v_p^2}{2T_{eF}} \right)^{1/2} = \left( \epsilon_p \frac{m_e c^2}{T_{eF}} \right)^{1/2} = 714.84 \left( \frac{\epsilon_p}{T_{eF,eV}} \right)^{1/2}, \quad (2.1.5)$$

$$T_{eF} = \left[ T_e^2 + \left( 2^{1/3} \pi \frac{\hbar^2}{m_e} n_{fe}^{2/3} \right)^2 \right]^{1/2} = \left\{ T_e^2 + \left[ \left( \frac{4}{3\sqrt{\pi}} \right)^{2/3} E_F \right]^2 \right\}^{1/2} = (T_e^2 + 0.68415 E_F^2)^{1/2}, \quad (2.1.6)$$

and

$$E_F = \frac{1}{2} m_e v_F^2 = \frac{\hbar^2}{2m_e} (3\pi^2 n_{fe})^{2/3} = 26.004 \left( \frac{\rho y_{tmol}}{A_{tmol}} \right)^{2/3} \quad [\text{eV}] \quad (2.1.7)$$

is the Fermi energy (non-relativistic). Transition from the Maxwellian case to the Fermi degenerate case is accomplished approximately by using  $T_{eF}$  from Eq. (2.1.6) instead of  $T_e$ . The weight coefficient  $(4/3\sqrt{\pi})^{2/3}$  in front of  $E_F$  ensures the Fermi-Teller [9] result (see also Ref. [10]) for the combination in front of the Coulomb logarithm in the limit of  $T_e \ll E_F$  with one and the same function  $G(x_e)$ , derived for the Maxwellian case. The accuracy of such a simple phenomenological interpolation between the Maxwellian and Fermi cases in the intermediate region, where  $T_e \simeq E_F$ , remains to be verified.

The Bohr-Bethe-Bloch theory was developed for  $\Lambda \gg 1$ , where the Coulomb logarithm  $L = \ln \Lambda$ . When target is a partially ionized plasma, we have the following  $\Lambda$  values for the free and bound electrons:

$$\Lambda_{fe} = \frac{2m_e v_{eF}^2 \gamma_{eF}^2 \exp(-\beta_{eF}^2)}{\hbar \omega_{pl} [1 + (1.781 y_p e^2 / \hbar v_{eF})^2]^{1/2}} = \frac{1.0220 \times 10^6 \beta_{eF}^2 \gamma_{eF}^2 \exp(-\beta_{eF}^2)}{(\hbar \omega_{pl})_{eV} (1 + 1.6892 \times 10^{-4} y_p^2 / \beta_{eF}^2)^{1/2}}, \quad (2.1.8)$$

$$\Lambda_{be,kij} = \frac{2m_e v_p^2 \gamma_p^2 \exp(-\beta_p^2)}{\hbar \bar{\omega}_{kij} [1 + (1.781 y_p e^2 / \hbar v_p)^2]^{1/2}} = \frac{1.0220 \times 10^6 \beta_p^2 \gamma_p^2 \exp(-\beta_p^2)}{(\hbar \bar{\omega}_{kij})_{eV} (1 + 1.6892 \times 10^{-4} y_p^2 / \beta_p^2)^{1/2}}, \quad (2.1.9)$$

Here

$$\hbar \omega_{pl} = \hbar \left( \frac{4\pi e^2 n_{fe}}{m_e} \right)^{1/2} = 3.71328 \times 10^{-11} n_{fe}^{1/2} = 28.816 \left( \frac{\rho y_{tmol}}{A_{tmol}} \right)^{1/2} \quad [\text{eV}] \quad (2.1.10)$$

is the plasmon energy, and  $\hbar \bar{\omega}_{kij}$  is the mean excitation energy of the bound electrons in a subshell  $j$  of an ion  $i$  of the element  $k$ . Equations (2.1.9) and (2.1.8) provide interpolation between the Bohr and Bethe cases as discussed in section A A.1.

Following the suggestion of Ref. [13], in Eq. (2.1.8) the transition from the ‘‘supersonic’’ (dynamic screening,  $v_p \gg \max\{\sqrt{2T_e/m_e}; \sqrt{2E_F/m_e}\}$ ) to the ‘‘subsonic’’ (quasi-static screening,  $v_p \ll \max\{\sqrt{2T_e/m_e}; \sqrt{2E_F/m_e}\}$ ) motion of the projectile in the Maxwellian (Fermi) gas of the plasma electrons is described approximately by using  $\beta_{eF} \equiv v_{eF}/c, \gamma_{eF}$ , defined as

$$\epsilon_{eF} = \frac{T_{eF}}{m_e c^2} \eta(x_e) = 1.95695 \times 10^{-6} T_{eF,eV} \eta(x_e), \quad (2.1.11)$$

$$\gamma_{eF} = 1 + \epsilon_{eF}, \quad \beta_{eF}^2 = \epsilon_{eF} (2 + \epsilon_{eF}) \quad (2.1.12)$$

$$\eta(x) = 0.353 + x^2 \frac{2.34 + x^3}{11 + x^3}, \quad (2.1.13)$$

instead of  $\beta_p \equiv v_p/c, \gamma_p$ . The function  $\eta(x_e)$ , with  $x_e$  given by Eq. (2.1.5), reproduces to a good (10% in the values of  $\Lambda_{fe}$ ) accuracy this transition in the Maxwellian case as calculated by Hamada [11]. In the strongly degenerate case in the limit of  $v_p \ll v_F, e^2/\hbar v_p \ll 1$ , our value of  $\Lambda_{fe}$  is 10% lower than that of Ritchie [10]. In the intermediate range of  $T_e \simeq E_F, v_p \simeq v_F$ , the error of our approximation is not known, and may turn out to be as high as a factor of 1.5–2 in the values of the Coulomb logarithm  $L_{fe}$ .

**Future tasks:** 1. Introduce the exact Chandrasekhar function  $G(x_e, \psi_e)$  for arbitrary degree of degeneracy  $0 \leq \psi_e \leq \infty$ .

## 2. Shell corrections

When the quantity  $\Lambda_{be,kij}$  (or  $\Lambda_{fe}$ ) becomes comparable to, or less than 1, we enter the low-velocity regime where the corresponding stopping number  $L$  is no longer the Coulomb logarithm  $L = \ln \Lambda$ . For bound electrons this occurs when the projectile velocity  $v_p$  becomes comparable to, or smaller than the mean atomic velocity in the subshell  $j$ ; at this point, the contribution of the corresponding subshell  $j$  to the stopping power is strongly suppressed. Adequate description of such ‘‘turning off’’ of the target-atom subshells is a complex task in itself. We make provision for several options to approximately describe this effect, which we somewhat loosely call shell corrections.

**Option 0 (IFSP0W2=0).** The simplest option would be to use

$$L_{be,kij} = \begin{cases} \ln \Lambda_{be,kij}, & \Lambda_{be,kij} \geq 1, \\ 0, & \Lambda_{be,kij} < 1, \end{cases} \quad L_{fe} = \begin{cases} \ln \Lambda_{fe}, & \Lambda_{fe} \geq 1, \\ 0, & \Lambda_{fe} < 1. \end{cases} \quad (2.1.14)$$

**Option 1 (IFSP0W2=1).** In this option we make use of the rigorous low-velocity solution for the Bohr model of a classical harmonically bound electron, reproduced by Eqs. (38) and (40) in Ref. [12]. The relation

$$\bar{v}_p^3 = \frac{1}{2} \exp(\gamma_E) \Lambda = 0.890536 \Lambda \quad (2.1.15)$$

between the dimensionless projectile velocity  $\bar{v}_p$  of Ref. [12] and parameter  $\Lambda$  is easily established by considering the limit of  $v_p \ll c, y_p e^2 / \hbar v_p \gg 1$ ; here  $\gamma_E = 0.5772 \dots$  is Euler’s constant.

Then, the stopping number  $L$  is given by the expressions

$$L = \begin{cases} \left( 1 + \frac{3\pi}{2} \frac{\bar{v}_p^{-3} (1.2 + \bar{v}_p)}{1 + \bar{v}_p} \right) \ln \left( 1 + \frac{1.122919 \bar{v}_p^6}{6.7696 + \bar{v}_p^3} \right), & Z_p > 0, \\ \frac{\ln(6.5528 + 1.122919 \bar{v}_p^3)}{1 + (3\pi/2) \bar{v}_p^{-3} + 2.36 \bar{v}_p^{-4} \exp(-5\bar{v}_p^2)}, & Z_p < 0, \end{cases} \quad (2.1.16)$$

depending on whether the projectile is an ordinary nucleus ( $Z_p > 0$ ) or an antinucleus ( $Z_p < 0$ ). In this way the Barkas effect is fully accounted for. By replacing  $\Lambda$  in Eq. (2.1.15) with  $\Lambda_{be,kij}$  (or  $\Lambda_{fe}$ ), we calculate from Eq. (2.1.16) the corresponding stopping number  $L_{be,kij}$  (or  $L_{fe}$ ).

### 3. Mean excitation energies $\hbar\bar{\omega}_{kij}$

For single-electron dipole transitions the quantities  $\hbar\bar{\omega}_{kij}$  and  $\tilde{n}_{kij}$  are defined as

$$\ln(\hbar\bar{\omega}_{kij}) = \frac{\sum_{j'} f_{ki,j \rightarrow j'} \ln(\hbar\omega_{ki,j \rightarrow j'})}{\tilde{n}_{kij}}, \quad \tilde{n}_{kij} = \sum_{j'} f_{ki,j \rightarrow j'}, \quad (2.1.17)$$

where  $f_{ki,j \rightarrow j'}$  and  $\omega_{ki,j \rightarrow j'}$  are, respectively, the oscillator strengths and the frequencies of all possible transitions leaving a hole in the electronic subshell  $j$ . In the code we use a representation

$$\hbar\bar{\omega}_{kij} = g_{kij} \epsilon_{kij}, \quad (2.1.18)$$

where  $\epsilon_{kij}$  is the binding energy of the subshell  $j$  of the ion  $i$  of the element  $k$ , and  $g_{kij}$  is a dimensionless coefficient of the order of 1.

Option 1 (IFSPOW1=1). In this option, the binding energies  $\epsilon_{kij}$  of ions  $i = 1$  (neutral atom) to  $i = Z_k$  (hydrogen-like ion) are evaluated approximately as

$$\epsilon_{kij} = \epsilon_{k1j} + (I_{ki} - \epsilon_{k1j_{ext,ki}}), \quad j = 1, 2, \dots, j_{ext,ki}, \quad (2.1.19)$$

where  $\epsilon_{k1j}$  are the known binding energies of the neutral atom,  $I_{ki}$  is the ionization potential of ion  $i$  of the element  $k$ , and  $j_{ext,ki}$  is the sequential number of the outermost subshell in the ion  $i$  of the element  $k$ .

To evaluate  $\hbar\bar{\omega}_{kij}$ , we use a phenomenological approach based on the observation that the mean excitation energies  $\hbar\bar{\omega}_{kij}$  are not much different from the binding energies  $\epsilon_{kij}$  (for hydrogen-like ions  $\hbar\bar{\omega}_{kij} = 1.102\epsilon_{kij}$  [5, 29]). First of all, we assume that  $g_{kij} = g_{ki}$  do not depend on  $j$ . Then, we use a simple interpolation,

$$\ln g_{ki} = \ln g_{ki1} + (\ln 1.102 - \ln g_{ki1}) \frac{i-1}{Z_k-1}, \quad (2.1.20)$$

to calculate  $\ln g_{ki}$  from the known value of  $\ln g_{ki1}$  for the neutral atom, which, in its turn, is evaluated as

$$\ln g_{ki1} = \ln(\hbar\bar{\omega}_{k1}) - \frac{\sum_j \tilde{n}_{k1j} \ln \epsilon_{k1j}}{\sum_j \tilde{n}_{k1j}} \quad (2.1.21)$$

from the known (mostly empirically, [4]) mean excitation energy of the neutral atom  $\hbar\bar{\omega}_{k1}$ .

Option 2 (IFSPOW1=2). This is the same as option 1 except that, instead of the crude interpolation (2.1.20), the values of  $g_{ki}$  are calculated as

$$\ln g_{ki} = \ln(\hbar\bar{\omega}_{ki}) - \frac{\sum_j \tilde{n}_{kij} \ln \epsilon_{kij}}{\sum_j \tilde{n}_{kij}} \quad (2.1.22)$$

from the known (from more accurate atomic calculations) values of  $\hbar\bar{\omega}_{ki}$ . If some needed values of  $\hbar\bar{\omega}_{ki}$  are not present in the database, the code issues a warning and calculates them according to option 1.

Option 3 (IFSPOW1=3). Here the values of  $\epsilon_{kij}$  and  $\hbar\bar{\omega}_{kij}$  are assumed to be known from separate atomic calculations, and are taken from the atomic database. If some needed values of  $\epsilon_{kij}$  or  $\hbar\bar{\omega}_{kij}$  are not present in this database, the code issues a warning and calculates them according to option 1.

## 2.2. Electronic stopping of neutral projectiles

### 1. Stopping on target atoms and ions

Among other possible effects, there is an obvious contribution to the stopping of neutrals on target ions (atoms): when a neutral atom, moving with a velocity  $v_p$ , ionizes a cold target ion (atom)  $ki$ , it loses at least an energy  $I_{tki}$  – the ionization potential of the target ion  $ki$ . In reality it loses more than that because (i) the freed electron has some kinetic energy, and (ii) the projectile atom and target ion may exit the collision in excited states.

The situation is less clear in the case when the neutral projectile is ionized itself in a collision with a target ion: here the ionized projectile may either lose some energy (when, for example, the projectile-bound electron is ejected into continuum) on the order of  $I_{p1}$  (the ionization potential of the neutral projectile), or even gain some energy (when, for example, the projectile-bound electron jumps over into a deeper potential well of a target ion). Clearly, in slow ( $v_p \ll v_0$ ) ionizing collisions with neutral target atoms a neutral projectile loses at least an energy  $I_{p1}$ . Somewhat arbitrarily, we assume that this is true for any collision with a target ion, in which the neutral projectile is ionized. Then, we evaluate the stopping power of neutral projectiles on bound target electrons as

$$\begin{aligned} -\frac{dE_p}{dx} &= g_{s0} \left[ \sum_{k,i} n_{ki} (I_{tki} \sigma_{itp0,ki} + I_{p1} \sigma_{i,ki}) \right] = \\ &= g_{s0} \frac{\rho}{16.6054 A_{tmol}} \sum_{k,i} \nu_k c_{tki} (I_{tki} \sigma_{itp0,ki} + I_{p1} \sigma_{i,ki}) \left[ \frac{\text{MeV}}{\text{cm}} \right]. \end{aligned} \quad (2.2.1)$$

Here  $g_{s0}$  is a numerical (fitting) factor of the order of 1 (typically, between 1 and 2),  $I_{tki}$  [eV] is the ionization potential of the ( $ki$ )-th target ion,  $I_{p1}$  [eV] is the first ionization potential of the projectile atom,  $\sigma_{itp0,ki}$  [ $10^{-19}$  cm $^2$ ] is the cross-section of ionization of the target ion  $ki$  by the neutral projectile atom, and  $\sigma_{i,ki}$  [ $10^{-19}$  cm $^2$ ] is the cross-section of ionization of the neutral projectile in collisions with the target ions  $ki$  — the same as in Eq. (4.0.7) for the charge exchange rate  $\kappa_i$ ; here the ionization cross-sections should not be mixed with the total cross-sections of electron loss.

### 3. ENERGY STRAGGLING

As a measure of the energy straggling, the quantity

$$\Omega_p^2 = \langle (E_p - \langle E_p \rangle)^2 \rangle \quad (3.0.2)$$

is used. In the Fokker-Planck approximation and for a  $\delta$ -like initial distribution over  $E_p$  we have

$$\frac{d\Omega_p^2}{ds} = 2D_E, \quad (3.0.3)$$

where  $D_E = v_p D_{\parallel}$  is the diffusion coefficient for the projectile distribution function along the energy axis  $E_p$ ,  $D_{\parallel}$  is the longitudinal diffusion coefficient in the momentum space,  $s$  is the distance along the projectile trajectory.

The diffusion coefficient  $D_E$  can be split into the electron and ion components,

$$D_E = D_{E,el} + D_{E,i}. \quad (3.0.4)$$

The contribution to  $D_E$  due to the Coulomb scattering on slow (*is this important for free electrons ???*) electrons (Bohr, 1915) can be written as

$$\begin{aligned} D_{E,el} &= 2\pi e^4 y_{p,Del}^2 (n_{fe} + n_{be}) \left( \frac{m_u A_p}{m_e + m_u A_p} \right)^2 \approx 2\pi e^4 y_{p,Del}^2 (n_{fe} + n_{be}) \\ &= 0.0784575 y_{p,Del}^2 \frac{\rho}{A_{tmol}} \sum_k \nu_k Z_{tk} \quad [\text{MeV}^2/\text{cm}]. \end{aligned} \quad (3.0.5)$$

Here  $y_p \leq y_{p,Del} \leq Z_p$  is an effective charge of the projectile for calculating  $D_{E,el}$ . Generally it will be higher than  $y_p$  because the main contribution to  $D_{E,el}$  comes from large transferred momenta (close to  $q_{max} = 2mv_p$ ), when the field electrons penetrate inside (but not deeply inside) the electron cloud around the projectile nucleus. Having no suitable theory for evaluating  $y_{p,Del}$ , we will use  $y_p$  instead.

**Problem:** Develop a model for evaluating  $y_{p,Del} = y_{p,Del}(y_p, v_p, Z_p)$ .

The contribution due to scattering on ions can be evaluated as (Bohr, 1915)

$$\begin{aligned} D_{E,i} &= 2\pi e^4 Z_p^2 \sum_k \frac{n_k Z_{tk}^2}{(1 + A_{tk}/A_p)^2} = 2\pi e^4 Z_p^2 \frac{\rho}{m_u A_{tmol}} \sum_k \frac{\nu_k Z_{tk}^2}{(1 + A_{tk}/A_p)^2} \\ &= 0.0784575 Z_p^2 \frac{\rho}{A_{tmol}} \sum_k \frac{\nu_k Z_{tk}^2}{(1 + A_{tk}/A_p)^2} \quad [\text{MeV}^2/\text{cm}]. \end{aligned} \quad (3.0.6)$$

Again, because the main contribution to  $D_{E,i}$  comes from large transferred momenta (close to  $q_{max} = 2mv_p$ , where  $m$  is the reduced mass), when the nuclei of colliding ions penetrate deeply inside (approach distances on the order of  $10^{-13}$  cm) their electron shells, we use the charges of bare nuclei in the Bohr formula.

Note that neither  $D_{E,el}$  nor  $D_{E,i}$  depend on the relative velocity between the projectile ion and the target particle.

### 4. CHARGE CHANGE RATES

In general, for each projectile charge state  $m$  we calculate two charge-change rate coefficients due to collisions with free electrons and partially ionized ions (atoms) in the target, namely, the coefficient of ionization (or, in other words, the coefficient of electron loss),

$$\kappa_i = \sigma_{i,fe} n_{fe} + \sum_k \sum_i \sigma_{i,ki} n_{ki} = 6.02214 \times 10^4 \frac{\rho}{A_{tmol}} \left( \sigma_{i,fe} y_{tmol} + \sum_k \sum_i \sigma_{i,ki} \nu_k C_{tki} \right), \quad (4.0.7)$$

and the coefficient of recombination,

$$\kappa_r = \sigma_{r,fe} n_{fe} + \sum_k \sum_i \sigma_{r,ki} n_{ki} = 6.02214 \times 10^4 \frac{\rho}{A_{tmol}} \left( \sigma_{r,fe} y_{tmol} + \sum_k \sum_i \sigma_{r,ki} \nu_k C_{tki} \right); \quad (4.0.8)$$

here  $\sigma_{i,fe}$  ( $\sigma_{r,fe}$ ) is the ionization (recombination) cross-section [in  $10^{-19}$  cm<sup>2</sup>] of the projectile ion  $m$  in collisions with the free target electrons, and  $\sigma_{i,ki}$  ( $\sigma_{r,ki}$ ) is the ionization (recombination) cross-section [in  $10^{-19}$  cm<sup>2</sup>] of the projectile ion  $m$  in collisions with the target ions  $ki$ ; index  $m$  for the quantities  $\kappa_i$ ,  $\kappa_r$ ,  $\sigma_{i,fe}$ ,  $\sigma_{r,fe}$ ,  $\sigma_{i,ki}$ ,  $\sigma_{r,ki}$  is omitted; the rates  $\kappa_i$ ,  $\kappa_r$  are in units of cm<sup>-1</sup>. It is convenient to calculate the cross-sections in the reference frame comoving with the projectile, where the velocity of the target particles is  $v_p$  (the thermal motion of the free target electrons is only crudely accounted for the moment; see below). In atomic units, the dimensionless projectile velocity is given by

$$\tilde{v}_p = \frac{v_p}{v_0}, \quad \text{where} \quad v_0 = \frac{e^2}{\hbar} = 2.187691417(98) \times 10^8 \text{ cm/s}; \quad (4.0.9)$$

we use also the equivalent electron energy

$$E_{eeq} = \frac{m_e}{m_u} \frac{E_p}{A_p} = 548.580 \frac{E_{p,MeV}}{A_p} \quad [\text{eV}]. \quad (4.0.10)$$

When evaluating the cross-sections, we always use the non-relativistic approximation, for which

$$E_{eeq} = \frac{1}{2} m_e v_p^2 = \text{Ry} \cdot \tilde{v}_p^2, \quad \text{where} \quad \text{Ry} = \frac{1}{2} m_e v_0^2 = 13.6056981(40) \text{ eV}, \quad (4.0.11)$$

$$E_{p,MeV} = 0.02480167 \tilde{v}_p^2 A_p, \quad \tilde{v}_p = 6.349793 \sqrt{E_{p,MeV}/A_p}.$$

When calculating the charge change rates, thermal motion of atoms and plasma ions is ignored, whereas the thermal motion of the free electrons is taken into account only crudely, by using an effective value

$$E_{eeq,ef} = E_{eeq} + \frac{3}{2} T_e \quad (4.0.12)$$

instead of  $E_{eeq}$  in the corresponding cross-section subroutines; the latter means that, instead of  $v_p$ , we use the value  $\sqrt{v_p^2 + 3T_e/m_e}$  for the relative velocity of collisions with the free plasma electrons.

## 5. CROSS-SECTIONS: PROJECTILE IONIZATION IN COLLISIONS WITH FREE ELECTRONS

### 5.1. Theory-1 option: the Lotz formula

As a universal theoretical formula for ionization cross-section in collisions with free electrons, the Lotz formula [14, 15] is adopted.

## 6. CROSS-SECTIONS: PROJECTILE RECOMBINATION IN COLLISIONS WITH FREE ELECTRONS

### 6.1. Theory-1 option: a simple and universal theoretical model

Here we take into account the radiative and the three-body recombination processes,

$$\sigma_{re} = \sigma_{rer} + \sigma_{re3}. \quad (6.1.1)$$

For the cross-section of radiative recombination we adopt the Kramers formula, originally derived for the hydrogen-like ions [37, vol. I, ch. V, § 4],

$$\sigma_{rer} = \frac{32\pi}{3\sqrt{3}} \alpha^3 a_0^2 \frac{I_{pm}}{E_{eeq,ef}} \varphi\left(\frac{I_{pm}}{E_{eeq,ef}}\right) = 2.105 \times 10^{-22} \frac{I_{pm}}{E_{eeq,ef}} \varphi\left(\frac{I_{pm}}{E_{eeq,ef}}\right) \text{ cm}^2, \quad (6.1.2)$$

where  $\alpha = e^2/\hbar c$  is the fine structure constant,  $a_0 = \hbar^2/m_e e^2$  is the Bohr radius,  $I_{pm}$  is the ionization potential of the projectile in charge state  $m$ ,  $E_{eeq,fe} = \frac{1}{2} m_e v_p^2 + \frac{3}{2} T_e$  is the effective electron energy in the projectile reference frame, and the function  $\varphi(x)$  is given by

$$\varphi(x) = \sum_{n=1}^{\infty} \frac{1}{n(1+n^2/x)} \approx \frac{1}{2} \ln(1+2.5x). \quad (6.1.3)$$

Generalization from the original Kramers formula to Eq. (6.1.2) is performed by replacing the hydrogen-like ionization potential  $Z^2 \text{ Ry}$  with  $I_{pm}$  and using  $E_{eeq,fe}$  instead of  $\frac{1}{2} m_e v_p^2$ .

For the cross-section of three-body recombination we assume a simple estimate from [37, vol. I, ch. VI, § 17], obtained for a hydrogen-like ion,

$$\sigma_{re3} = 32\pi^2 \frac{a_0^5}{\tilde{v}_{p,ef}^{10}} q_m^3 n_e = 8.844 \times 10^{-15} q_m^3 \left(\frac{\text{Ry}}{E_{eeq,ef}}\right)^5 \left(\frac{\rho}{11.206 \text{ g/cc}}\right) \frac{y_{tmol}}{A_{tmol}} \text{ cm}^2, \quad (6.1.4)$$

where  $q_m$  is the electric charge (in atomic units) of the projectile in charge state  $m$ , and  $\tilde{v}_{p,ef}^2 = \tilde{v}_p^2 + 3T_e/2\text{Ry}$ .

## 7. CROSS-SECTIONS: PROJECTILE IONIZATION IN COLLISIONS WITH TARGET IONS (ATOMS)

### 7.1. Theory-1 option: a universal theoretical model for ionization into continuum

Here we consider the process of projectile ionization in collisions with partially ionized target ions (atoms), where a bound projectile electron is ejected into the continuum:

$$Z^{q+} + Z_t^{q_t+} \longrightarrow Z^{(q+1)+} + Z_t^{q_t+} + e^-. \quad (7.1.1)$$

We call the corresponding cross-section  $\sigma_{ia,c}$  the cross-section of *ionization into continuum*. The total cross-section of projectile ionization in collisions with target ions (atoms) will then be given by

$$\sigma_{ia} = \sigma_{ia,c} + \sigma_{ia,b}, \quad (7.1.2)$$

where  $\sigma_{ia,b}$  is the cross-section of electron transfer from projectile into the vacant bound states of the target ions  $Z_t^{q_t+}$  (see section 8.8.1). We assume that  $\sigma_{ia,c}$  is the *direct* ionization cross-section and ignore the additional contribution to the electron loss due to the Auger cascades following direct ionization from the inner shells. On the one hand, this would be a natural simplification because we are looking for a practical universal formula valid for any combination of the projectile and target ions (atoms): one cannot demand too high an accuracy from such a formula. On the other hand, the dominant contribution to  $\sigma_{ia,c}$  comes always from the outer shells, for which the Auger cascades either do not exist or are not particularly important.

To comply with the conventional terminology in this field (especially, when comparing with the results of other authors), from now on in this paragraph we change the notation and call the ionizing ion (atom) a ‘*projectile*’ ion, and the ion (atom) undergoing ionization a ‘*target*’ ion, i.e. we analyze the ionization event

$$Z^{q+} + Z_t^{q_t+} \longrightarrow Z^{q+} + Z_t^{(q_t+1)+} + e^-. \quad (7.1.3)$$

We omit for brevity the index  $p$  for the parameters of the ‘projectile’ ion — such as its atomic number  $Z$ , charge  $q$ , and velocity  $v$ . The electron shells of the ionized ‘target’ ion of atomic number  $Z_t$  and charge  $q_t$  are labeled  $nl$ , with the corresponding binding energies  $\epsilon_{nl}$  and the number of the electrons in each shell  $N_{nl}$ .

**Fully stripped ionizing ions.** We begin with the simpler case of a fully stripped point-charge ionizing ion  $q = Z$ , for which the following scaling formula has recently been proposed by Kaganovich *et al.* [16]:

$$\sigma_{ia,c} = 2\pi a_0^2 \frac{q^2}{\tilde{v}^2} \sum_{nl} \frac{N_{nl}}{\tilde{\epsilon}_{nl}} G\left(\frac{\tilde{v}}{\tilde{v}_{nl}\sqrt{q+1}}\right). \quad (7.1.4)$$

Here  $a_0 = \hbar^2/m_e e^2 = 0.529177249(24) \times 10^{-8}$  cm is the Bohr radius,  $\tilde{v}$  is the projectile velocity in the atomic units,  $\tilde{\epsilon}_{nl} = \epsilon_{nl}/(m_e v_0^2)$  is the electron binding energy of the ionized ion shell  $nl$  in the atomic units of  $m_e v_0^2 = e^2/a_0 = 27.2113961(81)$  eV,  $\tilde{v}_{nl} = v_{nl}/v_0 = (2\tilde{\epsilon}_{nl})^{1/2}$  is the corresponding atomic velocity [in the atomic units of  $v_0 = e^2/\hbar = 2.187691417(98) \times 10^8$  cm/s],  $N_{nl}$  is the number of bound electrons in the corresponding shell  $nl$ ,  $q = Z$  is the charge of the ionizing ion (in atomic units), and  $G(x)$  is the adiabatic/quantum correction factor. For  $G = 1$  and a fixed shell  $nl$ , we recover from Eq. (7.1.4) the classical Thomson [17] cross-section

$$\sigma_{Th} = \frac{2\pi e^4 q^2 N_{nl}}{m_e v^2 \epsilon_{nl}} = 2\pi a_0^2 \frac{q^2}{\tilde{v}^2} \frac{N_{nl}}{\tilde{\epsilon}_{nl}} \quad (7.1.5)$$

of ionization from a shell  $nl$  of the ‘target’ ion. The factor  $G$  represents the quantum correction at  $v \gg v_{nl}$ , and the adiabatic correction at  $v \ll v_{nl}$ ; in a certain sense, it is analogous to the Gaunt factor in the theory of dipole radiative transitions and bremsstrahlung.

The Thomson cross-section (7.1.5) has a clear classical interpretation in the limit of  $v \gg v_{nl}$ : it is equal to  $\pi b^2$ , where  $b$  is the maximum impact parameter, for which the energy transfer in a single Coulomb collision of a heavy ‘projectile’ with a free electron at rest [3, §13.1],

$$\Delta E = \frac{(\Delta p)^2}{2m_e} = \frac{2e^4 q^2}{m_e v^2 b^2} \geq \epsilon_{nl}, \quad (7.1.6)$$

is still sufficient to eject the electron with a binding energy  $\epsilon_{nl}$ . For the correction factor  $G(x)$ , the authors of Ref. [16] have proposed the following expression,

$$G_{KSD}(x) = \exp\left(-\frac{1}{x^2}\right) [1.26 + 0.283 \ln(2x^2 + 25)] \quad (7.1.7)$$

(our definition of  $G$  is that of Ref. [16] multiplied by  $x^2$ ), which is a combination of the Bethe asymptotic result for  $x \gg 1$  and a fit to experimental data for  $x \lesssim 1$ .

Here we modify the  $G$  factor of Ref. [16] to the following expression,

$$G(x) = \exp\left(-\frac{1}{\sqrt{x^4 + 0.5x^2}}\right) [1.26 + 0.283 \ln(2x^2 + 25)]. \quad (7.1.8)$$

We see at least two compelling arguments for such a modification. First of all, from the theoretical point of view, the function  $G_{KSD}(x)$  falls off too fast in the limit of  $x \ll 1$ : in the adiabatic limit  $v \ll v_{nl}$  one would expect  $\sigma_{ia,c}$  to decrease as  $\sigma_{ia,c} \propto \exp(-C/v)$  with the decreasing  $v$  rather than  $\sigma_{ia,c} \propto \exp(-C/v^2)$  [18–20].

The second argument arises from a comparison with the experimental and theoretical data on the ionization of the K-shell of elements beyond helium. Kaganovich *et al.* have calibrated their  $G$  function against the experimental data for several fully stripped ‘projectiles’ (up to  $O^{8+}$ ), but only for the H and He ‘targets’. Aiming at a universal formula, a natural next step would be to fix the ‘projectile’ (protons) and calibrate the fitting formula against the ionization data for different atomic shells of different ‘target’ elements, up to the heaviest ones. A comprehensive study in this direction has been undertaken by McGuire [21], who actually calculated the values of  $G$  for different shells  $nl$  of different elements in the Born approximation and compared them to the available experimental data.

If we want a universal function  $G(x)$  for all shells, the K-shell data might be a good starting point. Calculations by McGuire indicate that the correspondingly rescaled data for higher  $nl$  shells typically do not differ much (15–30% near the cross-section maxima) from the  $1s$  values, although in some cases (for high- $l$  outer shells of heavy elements) the error of a universal scaling may amount to about a factor 3. Figure 7.1.1 shows the results for the  $1s$  shell from Ref. [21] compared with both the fit (7.1.7) by Kaganovich *et al.* (dotted curve) and the present fit (dashed curve). The present fit (7.1.8) agrees almost perfectly with both the calculations of McGuire and the experimental data (within the accuracy and scatter of the latter) for a wide selection of the target elements, from He to U.

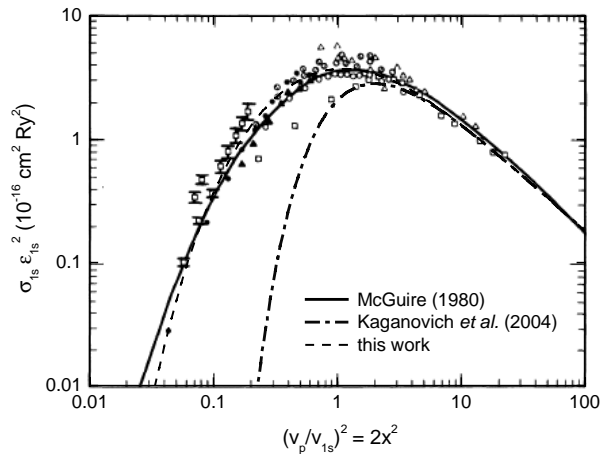


FIG. 7.1.1: Comparison with the scaled ionization cross-section data for the  $1s$  shell from Ref. [21]

**Comparison with experimental data for multi-electron target atoms.** When one tries to interpret the cross-section (7.1.4) in terms of classical trajectories (for  $v \gg v_{nl}$ , analogously to the logic behind the Thomson cross-section), one comes to a conclusion that for multi-electron ‘target’ atoms it should represent the total cross-section  $\sigma_- = \sum_i i\sigma_{ie}$  of the electron production [22] (here  $\sigma_{ie}$  is the ionization cross-section with simultaneous ejection of  $i$  electrons).

Figure 7.1.2 shows how our Eqs. (7.1.4) and (7.1.8) compare with the recommended values from Ref. [22] for the total electron production by protons in monoatomic noble gases. The latter have been obtained by critical analysis of numerous experimental results. One sees that generally a satisfactory agreement is observed near and beyond the cross-section maximum  $v \gtrsim v_{max}$ . At low relative velocities  $v < v_{max}$  Eqs. (7.1.4), (7.1.8) tend to overestimate the electron production cross-section for low- $Z$  elements, and to underestimate it for high- $Z$  elements. Note, however, that the experimental data at  $v < v_{max}$  tend to have significant scatter at  $v < v_{max}$ , as is illustrated in Fig. 7.1.2 with the data from Refs. [23] (ADFF) and [24] for He. Also, the estimated reliability of the recommended data in Ref. [22] at low velocities is rather low.

Here a remark should be made that, from the point of view of the beam stopping problem, large errors in the ionization cross-sections by strongly stripped ions at  $v < v_{max}$  have rather limited influence because this is the region where the charge transfer usually dominates over the direct ionization.

**Effective charge of the ionizing ion.** To generalize the cross-section (7.1.4), (7.1.8) established for fully stripped ‘projectiles’ with  $q = Z$  to an arbitrary ion  $Z^{q+}$ , we replace the charge  $q$  of a point-like projectile with an effective charge  $q_*$ , calculated on the basis of a static screening model described in Appendix B. For arguments justifying applicability of the static screening in this case one is referred to the paper by Bohr [25]. In doing so, we assume that the electron is ejected from the ‘target’ atom (ion) only due to interaction with the screened potential of the ‘projectile’ nucleus. Here we do not try to account for the contribution due to non-coherent collisions with the outer

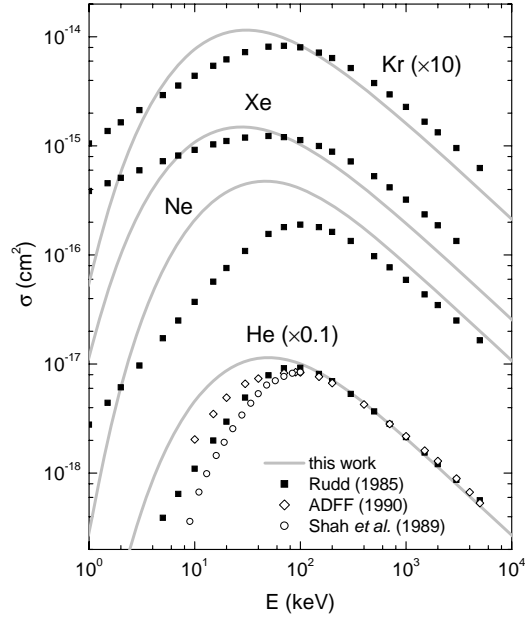


FIG. 7.1.2: Comparison with the total electron production cross-section by protons on multi-electron neutral atoms [22]

‘projectile’ electrons (which, in particular, result in  $\sigma_{ia,c} \propto Z^2 + Z$  instead of  $\sigma_{ia,c} \propto Z^2$  at  $v \gg v_{nl}$  [25]) because such a correction would be beyond the accuracy of the present model.

In the high velocity limit  $v \gg v_{nl}$ , the effective charge can be evaluated by natural generalization of the Thomson formula, namely, from the condition

$$\sigma_{ia,c} = \frac{2\pi e^4 q_*^2}{m_e v^2 \epsilon_{nl}} = \pi b^2, \quad (7.1.9)$$

where  $b$  is the maximum value of the impact parameter, for which the transferred momentum  $|\Delta p| \geq \sqrt{2m_e \epsilon_{nl}}$  is high enough to eject the bound  $nl$  electron into continuum. By using the value of  $|\Delta p|$  calculated in Appendix B as a function of the impact parameter  $b$ , we express the effective charge as

$$q_* = \bar{b} \frac{1}{2} \tilde{r}_a \tilde{v}_{nl}, \quad (7.1.10)$$

where  $\tilde{r}_a$  is the ‘projectile’ ion radius in atomic units [as given by Eq. (B.10)], and the parameter  $\bar{b} = b/r_a$  is found by solving the transcendental equation

$$\eta(\bar{b}) \equiv q + (Z - q) \frac{(1 - \bar{b})^2}{1 + \alpha \bar{b}} = \frac{\bar{b}}{\mu(\bar{b})} \frac{1}{2} \tilde{r}_a \tilde{v}_{nl}. \quad (7.1.11)$$

Here

$$\alpha = 0.53 \frac{\tilde{r}_a Z}{(Z - q)^{2/3}} - 2, \quad (7.1.12)$$

and the function  $\mu(\bar{b})$  is defined as

$$\mu(\bar{b}) = \begin{cases} \frac{\bar{q} + (1 - \bar{q}) \left[ \sqrt{1 - \bar{b}^2} - \bar{b}(\alpha + 2) \arcsin \sqrt{1 - \bar{b}^2 + \bar{b}^2(\alpha + 1)^2} \phi \right]}{\bar{q} + (1 - \bar{q})(1 - \bar{b})^2 / (1 + \alpha \bar{b})}, & 0 < \bar{b} < 1, \\ 1, & 1 \leq \bar{b}, \end{cases} \quad (7.1.13)$$

where  $\bar{q} = q/Z$ , and  $\phi = \phi(\alpha, \bar{b})$  is defined by Eq. (B.13). Equation (7.1.11) can be easily solved by successive iterations: first we assume  $\mu$  to be known ( $\mu = 1$  is a good zero approximation) and solve the quadratic equation (7.1.11) for  $\bar{b}$ ,

$$\bar{b} = \begin{cases} \left\{ \left\{ 1 - \bar{q} + \frac{1}{2}(\nu - \alpha \bar{q}) + \sqrt{(\nu - \bar{q})(\alpha + 1) + \left[ \bar{q} + \frac{1}{2}(\alpha \bar{q} - \nu) \right]^2} \right\}^2 \right\}^{-1}, & \nu > \bar{q}, \\ \bar{q}/\nu, & \nu < \bar{q}, \end{cases} \quad (7.1.14)$$

where

$$\nu = \frac{\tilde{r}_a \tilde{v} \tilde{v}_{nl}}{2\mu Z}; \quad (7.1.15)$$

then we calculate  $\mu$  from Eq. (7.1.13) and repeat the iteration. Usually 3–5 iterations are sufficient. Even the first iteration — as is illustrated by Fig. 7.1.3 — yields  $q_*$  to an accuracy better than 20%.

In the low velocity limit,  $v \rightarrow 0$ , the above formulae yield  $\bar{b} \rightarrow 1$ ,  $q_* \rightarrow 0$ , and the Thomson cross-section (7.1.9) approaches the geometric value  $\pi r_a^2$ . This would be physically reasonable, had we not already taken into account the adiabatic limit  $v \ll v_{nl}$  by means of the exponentially dropping factor  $G(x)$ . Clearly, for an ionization to occur in the adiabatic limit, the perturbing potential of the projectile at the location of the target electron should be at least of the order of its binding energy  $\epsilon_{nl}$ . The latter means that the effective charge in this limit should be evaluated with  $v \simeq v_{nl}$  rather than with  $v \ll v_{nl}$ . The latter is achieved by replacing the actual velocity  $v$  in Eqs. (7.1.9)–(7.1.11), and (7.1.15) with the effective velocity  $v_* = \sqrt{v^2 + v_{nl}^2}$ . As an example, the effective charge  $q_*$  for two Pb ions is plotted in Fig. 7.1.3 as a function of the product  $vv_{nl}$ .

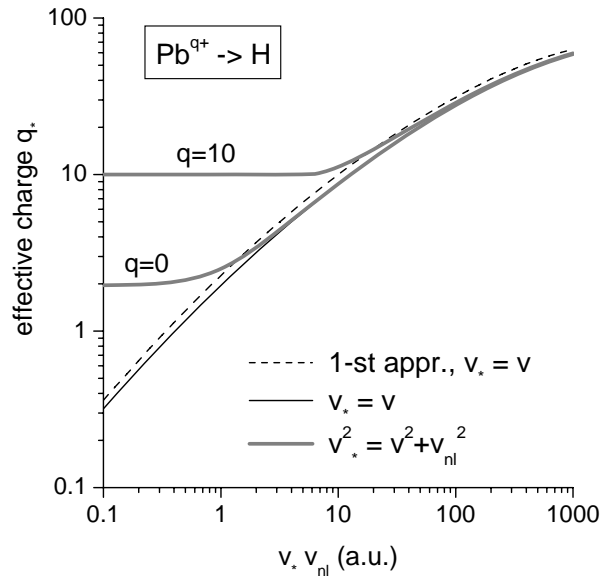


FIG. 7.1.3: Effective charge of  $\text{Pb}^{9+}$  projectiles as a function of the product  $v_* v_{nl}$  (in atomic units).

**Comparison with experimental data for multi-electron ‘projectile’ atoms.** The simplest test of our effective charge model would be to compare its predictions with the experimental cross-section for ionization of hydrogen atoms ( $N_{nl} = 1$ ,  $\tilde{\epsilon}_{nl} = \frac{1}{2}$ ,  $\tilde{v}_{nl} = 1$ ) in collisions with other multi-electron neutral atoms. Such data have mostly been obtained by measuring the ionization cross-section  $\sigma_{01}$  of H atoms in hydrogen beams propagating in various gases [26]. In our notation, we have to invert the terminology and call the H atoms the ‘target’ atoms, and the multi-electron ionizing atoms of gas the ‘projectile’ atoms with a specific (per nucleon) kinetic energy  $E_p$  equal to the hydrogen energy in the original experiments. The corresponding comparison with the compilation of the experimental data from Ref. [26] is shown in Figs. 7.1.4 and 7.1.5.

In these figures one sees that a fair agreement is observed around the cross-section maxima ( $v \simeq v_{max}$ ) for all elements, up to the heaviest ones, although the experimental data for the latter are rather scarce. At the same time, our model systematically overestimates the ionization cross-sections at higher velocities,  $v \simeq 3\text{--}10v_{max}$ , by a factor 2–4 with respect to the available experimental data. The reason for this systematic discrepancy is not quite clear because from the classical point of view the ionizing collisions at high velocities occur at small impact parameters (0.1–0.2 $a_0$  for He projectiles at  $E \simeq 2$  MeV/u), and the screening is already not important (at least for low-Z ‘projectiles’); hence, the cross-section should approach that for a fully stripped ion with the same  $Z$ . At least partly, the explanation may be due to the resonance energy transfer below the classical ionization threshold, as discussed by Bohr [25], that is much more pronounced for fully stripped projectiles (and manifests itself in the Bethe logarithmic correction to the Thomson cross-section) than for screened atoms.

## 7.2. Experiment-1 option:

### 1. Ionization of H projectiles in collisions with the $\text{H}_2$ molecules

Good accuracy measurements of the charge exchange cross-sections for protons and H atoms in different gases at projectile velocities  $v_p \gtrsim v_0$  have been reported in Refs. [28], [31]. We approximate their data for the electron loss by

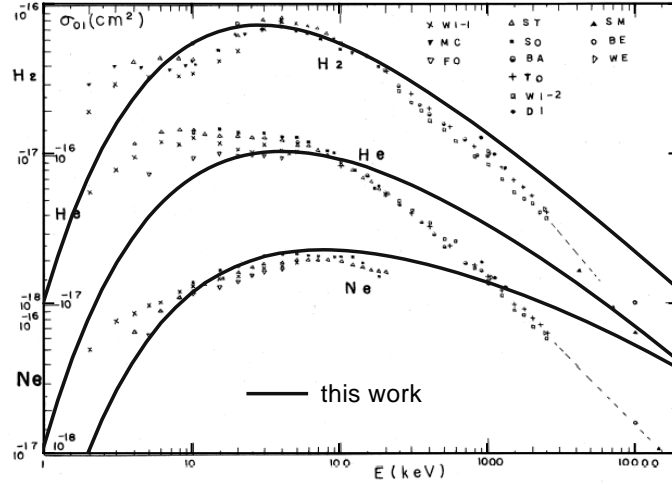


FIG. 7.1.4: Comparison with the experiments for ionization of hydrogen atoms in collisions with neutral  $H_2$ , He, and Ne from Ref. [26].

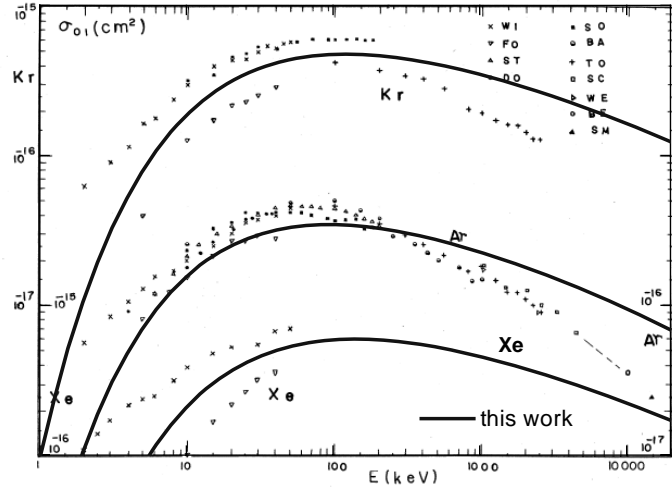


FIG. 7.1.5: Comparison with the experiments for ionization of hydrogen atoms in collisions with neutral Ar, Kr, and Xe from Ref. [26].

H atoms with velocity  $v_p$  in the the  $H_2$  gas as

$$\sigma_{iH,H_2}(v_p) = 3.6 \times 10^{-16} \frac{\tilde{v}_p^2}{1.7 + 1.9\tilde{v}_p^2 + \tilde{v}_p^4} \left[ \frac{\text{cm}^2}{\text{atom H}} \right]. \quad (7.2.1)$$

Note that this expression gives the cross-section of electron loss per H atom (and not per  $H_2$  molecule) of the  $H_2$  target. The accuracy of this interpolation is 3–5% in the velocity range  $2 \times 10^8 \text{cm/s} < v_p < 6 \times 10^8 \text{cm/s}$ , and 20–30% at velocities  $1 \times 10^8 \text{cm/s} < v_p < 1 \times 10^8 \text{cm/s}$ ,  $v_p \simeq 20 \times 10^8 \text{cm/s}$ .

## 2. Ionization of H projectiles in collisions with the $H^+$ ions

In this case the electron loss cross-section is the sum,

$$\sigma_{iH,H^+} = \sigma_- + \sigma_{ec}, \quad (7.2.2)$$

of the two cross-sections, namely, of the cross-section  $\sigma_-$  of the free electron production (ionization “proper”), and of the cross-section  $\sigma_{ec}$  of the charge exchange (electron capture) with the field proton  $H^+$ . The latter can be evaluated

as a particular case of the H target in the modified Phaneuf's [32] formula (8.2.17):

$$\sigma_{ec} = 1.193 \times 10^{-16} \frac{\ln(1 + 2.367 \times 10^4 / \tilde{v}_p^2)}{1 + 1.1767 \tilde{v}_p^4 + 0.2606 \tilde{v}_p^9} \left[ \frac{\text{cm}^2}{\text{ion H}^+} \right]. \quad (7.2.3)$$

The cross-section of the electron production can be sufficiently accurately evaluated from the approximate formula proposed by Rudd *et al.* [22]

$$\sigma_- = 3.519 \times 10^{-16} \left[ \frac{1}{0.44 \tilde{v}_p^{1.814}} + \frac{\tilde{v}_p^2}{0.28 \ln(1 + \tilde{v}_p^2) + 1.15} \right]^{-1} \left[ \frac{\text{cm}^2}{\text{ion H}^+} \right]. \quad (7.2.4)$$

### 3. Ionization of H projectiles in collisions with the O<sub>2</sub> molecules

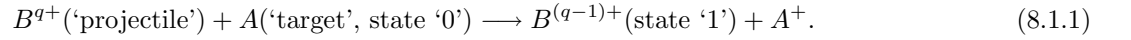
We approximate the experimental data from Refs. [28], [31] as

$$\sigma_{iH,O_2}(v_p) = 4.3 \times 10^{-15} \frac{\tilde{v}_p^2}{5.8 + 15.2 \tilde{v}_p^2 + \tilde{v}_p^4} \left[ \frac{\text{cm}^2}{\text{atom O}} \right]. \quad (7.2.5)$$

## 8. CROSS-SECTIONS: PROJECTILE RECOMBINATION IN COLLISIONS WITH TARGET IONS (ATOMS)

### 8.1. Theory-1 option: a universal theoretical model for the electron transfer in collisions between two ions

Here we consider the process of charge (electron) transfer from a bound state '0' of an ion (atom) *A* (a 'target' ion) to a bound state '1' of an ion  $Z^{(q-1)+}$ ,



We call the corresponding cross-section  $\sigma_{0 \rightarrow 1}$  the cross-section of electron transfer, see 77.1. The present model for evaluation of this cross-section is based on the Brinkman-Kramers formula adapted for non-hydrogenic ions according to the suggestions in Refs. [38, 39].

The total electron transfer cross-section is written as a sum over the subshells *j* of the 'target' ion *A*,

$$\sigma_{0 \rightarrow 1} = \pi a_0^2 \sum_j N_{0j} \tilde{\sigma}_{0j \rightarrow 1}, \quad (8.1.2)$$

where  $N_{0j}$  is the number of equivalent bound electrons in the subshell *j* of the 'target' ion *A*,  $\tilde{\sigma}_{0j \rightarrow 1}$  is the partial cross-section in atomic units. The Brinkman-Kramers formula (corrected by a factor 1/3 to agree with the Born-approximation results in the high-velocity limit [38, 39]),

$$\tilde{\sigma}_{0j \rightarrow 1n, BK} = \frac{2^8}{15 \tilde{v}^2} \frac{(2\tilde{\epsilon}_{1n})^{5/2} (2\tilde{\epsilon}_{0j})^{5/2} n^2}{[2\tilde{\epsilon}_{0j} + \tilde{v}^{-2}(\tilde{\epsilon}_{1n} + \frac{1}{2}\tilde{v}^2 - \tilde{\epsilon}_{0j})^2]^5}, \quad (8.1.3)$$

gives the cross-section of electron transfer to a hydrogen-like level of the 'projectile' ion  $B^{(q-1)+}$  with the principal quantum number *n* and the binding energy  $\tilde{\epsilon}_{1n}$ ; here  $\tilde{v} = v/v_0$  is the projectile velocity in atomic units. The partial cross-section  $\tilde{\sigma}_{0j \rightarrow 1}$  is obtained by summing  $\sigma_{0j \rightarrow 1n}$  up over all *n* values from  $n = n_1$  to  $n = \infty$ .

Because at low velocities  $\tilde{v} \lesssim 1$  Eq. (8.1.3) gives too high values of  $\sigma_{0j \rightarrow 1n}$ , we follow the suggestion of Ref. [39] [cf. Eqs. (13.40) and (13.42) in this book] and assume that  $\sigma_{0j \rightarrow 1n}$  should not exceed the value

$$\tilde{\sigma}_{0j \rightarrow 1n} \leq \tilde{\sigma}_{0j \rightarrow 1n, max} = \frac{K}{\gamma_{jn}^2} \exp\left(-\frac{\pi|\tilde{\epsilon}_{0j} - \tilde{\epsilon}_{1n}|}{\gamma_{jn}\tilde{v}}\right), \quad (8.1.4)$$

where

$$\gamma_{jn} = \frac{1}{2} \left( \sqrt{2\tilde{\epsilon}_{0j} + \frac{\tilde{v}^2}{4}} + \sqrt{2\tilde{\epsilon}_{1n} + \frac{\tilde{v}^2}{4}} \right), \quad (8.1.5)$$

and *K* is a universal constant of order unity ( $K = \pi^2/8$  in Ref. [39]) chosen for the best possible agreement with the experimental data. In practice, to ensure inequality (8.1.4), we use the formula

$$\tilde{\sigma}_{0j \rightarrow 1n} = \frac{\tilde{\sigma}_{0j \rightarrow 1n, BK} \tilde{\sigma}_{0j \rightarrow 1n, max}}{\tilde{\sigma}_{0j \rightarrow 1n, BK} + \tilde{\sigma}_{0j \rightarrow 1n, max}}. \quad (8.1.6)$$

The summation of  $\tilde{\sigma}_{0j \rightarrow 1n}$  over large values of  $n$  can be replaced by integration over

$$\tilde{\epsilon}_{1n} \equiv x_n = \frac{\tilde{\epsilon}_1 n_1^2}{n^2}, \quad (8.1.7)$$

(here  $\tilde{\epsilon}_1$  is the binding energy, and  $n_1$  the principal quantum number of the ground state of the ion  $B^{(q-1)+}$ ) — as it was proposed in Ref. [38].

Finally, we arrive at the following formulae for evaluation of  $\tilde{\sigma}_{0j \rightarrow 1}$ :

$$\tilde{\sigma}_{0j \rightarrow 1} = 2\tilde{\epsilon}_1 n_1^2 \sum_{n=n_1}^{n_1+n_{12}} \frac{1}{n^3} \phi(x_n) + \int_{\tilde{\epsilon}_{1min}}^{\tilde{\epsilon}_{12}} \phi(x) dx, \quad (8.1.8)$$

$$\phi(x) = \frac{\phi_{BK}(x) \phi_{VSY}(x)}{\phi_{BK}(x) + \phi_{VSY}(x)}, \quad (8.1.9)$$

$$\phi_{BK}(x) = \frac{2^8}{15\tilde{v}^2} \frac{(2\tilde{\epsilon}_1 n_1^2)^{3/2} (2\tilde{\epsilon}_{0j})^{5/2}}{[2\tilde{\epsilon}_{0j} + \tilde{v}^{-2}(x + \frac{1}{2}\tilde{v}^2 - \tilde{\epsilon}_{0j})^2]^5}, \quad (8.1.10)$$

$$\phi_{VSY}(x) = \frac{K}{2x\gamma_{jx}^2} \left( \frac{\tilde{\epsilon}_1 n_1^2}{x} \right)^{1/2} \exp\left(-\frac{\pi|\tilde{\epsilon}_{0j} - x|}{\gamma_{jx}\tilde{v}}\right), \quad (8.1.11)$$

$$\gamma_{jx} = \frac{1}{2} \left( \sqrt{2\tilde{\epsilon}_{0j} + \frac{\tilde{v}^2}{4}} + \sqrt{2x + \frac{\tilde{v}^2}{4}} \right), \quad (8.1.12)$$

$$\tilde{\epsilon}_{12} = \frac{\tilde{\epsilon}_1 n_1^2}{(n_1 + n_{12} + \frac{1}{2})^2}. \quad (8.1.13)$$

Typically the sum in Eq. (8.1.8) is taken over the three lowest levels, i.e. with  $n_{12} = 2$ . Integration in Eq. (8.1.8) is performed not from  $x = 0$  to  $x = \tilde{\epsilon}_{12}$  but rather from  $x = \tilde{\epsilon}_{1min} > 0$  with the consideration that very high levels either do not exist in dense targets, or are quickly ionized again before having time to relax to the ground state. In practice, the results depend very weakly on the value of  $\tilde{\epsilon}_{1min}$  once we have  $\tilde{\epsilon}_{1min} \ll 1$ ; as a typical value, we use  $\tilde{\epsilon}_{1min} = 0.1$ . As to the value of the fit parameter  $K$ , a good agreement with the experimental data was observed for  $K = 5$ .

One can easily verify that Eqs. (8.1.8)–(8.1.13) imply the following scaling for the maximum (with respect to  $\tilde{v}$ ) of the cross-section  $\tilde{\sigma}_{0j \rightarrow 1}$ ,

$$\tilde{\sigma}_{0j \rightarrow 1, max} \propto \frac{\tilde{\epsilon}_1}{\tilde{\epsilon}_{0j}^2} n_1^2 \propto \frac{q^2}{\tilde{\epsilon}_{0j}^2}, \quad (8.1.14)$$

if one assumes that  $q^2 = 2\tilde{\epsilon}_1 n_1^2$ . Note that for non-hydrogenic ions the value of  $n_1$  is, strictly speaking, undefined. Our logic behind assuming  $q^2 = 2\tilde{\epsilon}_1 n_1^2$  is that, when establishing a correspondence between hydrogenic and real non-hydrogenic states, we want the mean atomic velocities of the corresponding states to be the same.

## 8.2. Theory-2 option: Phaneuf *et al.* formula for the electron transfer

### 1. Recombination of arbitrary ions in collisions with the $H_2$ molecules, $H$ and $He$ atoms

In Ref. [32] a universal formula

$$\sigma_{rq^+, H_2}(E) = \frac{Aq \ln(B\sqrt{q}/E)}{1 + CE^2/q + D(E/\sqrt{q})^{4.5}} \quad (8.2.15)$$

was proposed for the cross-section of the charge-exchange reaction



where  $E$  [keV/u] is the kinetic energy of the projectile  $Z^{q+}$ , and  $A, B, C, D$  are fitting parameters. The semi-empirical formula (8.2.15) is based to a great extent on the scaling  $\sigma_{q, q-1}/q = f(E/q^{4/7})$  derived by Knudsen *et al.* [33] on the basis of the Bohr-Linhard model for  $q \gg 1$ . We have found that Eq. (8.2.15) also agrees well with the experimental data of Refs. [28], [31] for protons ( $q = 1$ ) when we slightly change it from  $\sigma_{q, q-1}/q = f(E/q^{0.5})$  to  $\sigma_{q, q-1}/(q+1) = f(E/q^{0.5})$ . This amendment leads also to a better agreement with the experimental data for  $O^{+3}$  (and extrapolated  $O^{+2}$ ) ions from Ref. [34]. Finally, we adopt the following semi-empirical formula,

$$\sigma_{rq^+, H_2}(v_p) = \frac{a(q+1) \ln[1 + b(q^{1/4}/\tilde{v}_p)^2]}{1 + c(\tilde{v}_p/q^{1/4})^4 + d(\tilde{v}_p/q^{1/4})^9} \left[ \frac{\text{cm}^2}{\text{atom H}} \right], \quad (8.2.17)$$

where the fitting coefficients  $a, b, c, d$ , as renormalized from  $A, B, C, D$  in Ref. [32], are given in Table I.

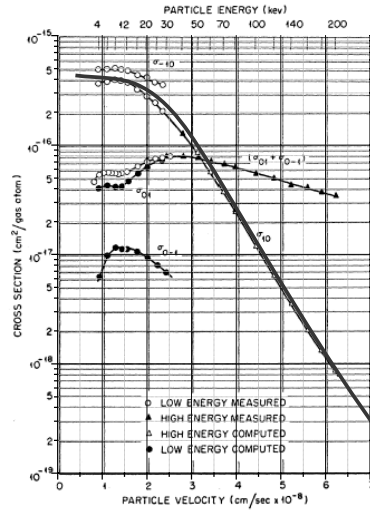


FIG. 8.1.1: Electron capture by protons in molecular hydrogen: comparison of the BKVSY model (thick grey curve) with the experimental data from Ref. [28].

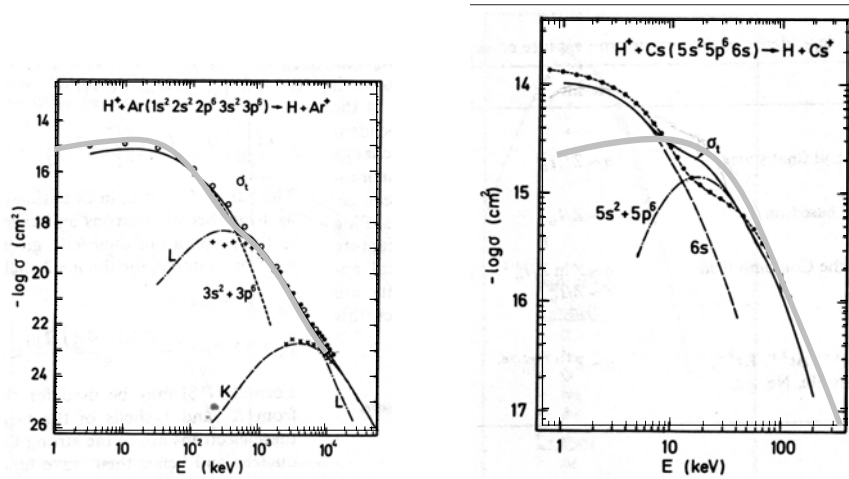


FIG. 8.1.2: Electron capture by protons in argon and cesium: comparison of the BKVSY model (thick grey curves) with the experimental data and other models as cited in Ref. [38].

### 8.3. Experiment-1 option:

#### 1. Recombination of protons in collisions with the $H_2$ molecules

My approximation of the experimental data from Refs. [28], [31] is

$$\sigma_{rH^+,H_2}(v_p) = \frac{4.5 \times 10^{-16}}{1 + 0.09 \tilde{v}_p^2 + 0.64 \tilde{v}_p^4 + 0.09 \tilde{v}_p^8 + 0.0005 \tilde{v}_p^{12}} \left[ \frac{\text{cm}^2}{\text{atom H}} \right]. \quad (8.3.18)$$

TABLE I: The values of the fitting parameters in Eq. (8.2.17).

Target	$a$	$b$	$c$	$d$
H	$5.967 \times 10^{-17}$	$2.367 \times 10^4$	1.1767	0.2606
$H_2$	$2.853 \times 10^{-17}$	$2.130 \times 10^3$	0.4798	$5.127 \times 10^{-2}$
He	$1.818 \times 10^{-17}$	$7.483 \times 10^4$	0.16934	$2.582 \times 10^{-3}$

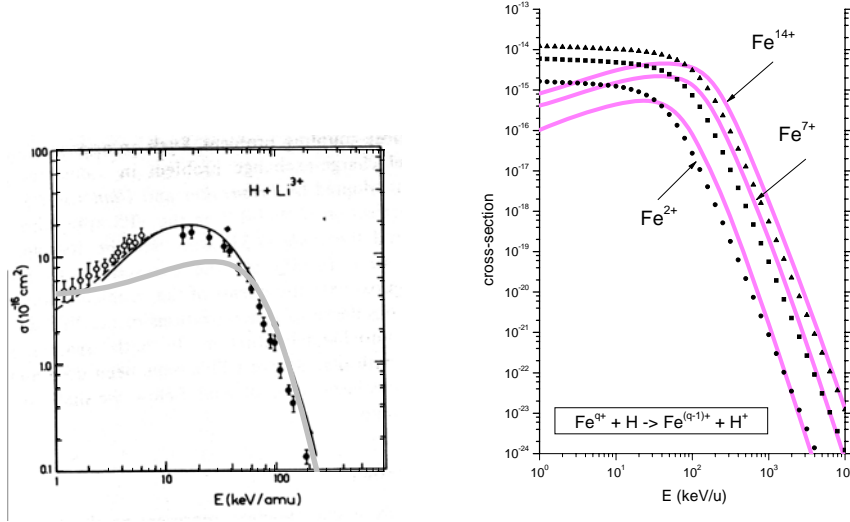


FIG. 8.1.3: Electron capture by Fe ions in hydrogen: comparison of the BKVSY model (thick grey curves) with the semi-empirical formula from Ref. [32].

Note that this expression gives the recombination cross-section per H atom (and not per H<sub>2</sub> molecule) of the H<sub>2</sub> target. The accuracy of this interpolation is 5–10% in the velocity range  $10^8 \text{ cm/s} < v_p < 16 \times 10^8 \text{ cm/s}$ .

## 2. Recombination of protons in collisions with the O<sub>2</sub> molecules

We approximate the experimental data from Refs. [28], [31] as

$$\sigma_{rH^+,O_2}(v_p) = \frac{5.6 \times 10^{-16}}{1 + 0.95 \tilde{v}_p^2 + 0.033 \tilde{v}_p^4 + 0.083 \tilde{v}_p^6 + 0.0033 \tilde{v}_p^8} \left[ \frac{\text{cm}^2}{\text{atom O}} \right]. \quad (8.3.19)$$

## 9. INITIAL CONDITIONS FOR THE DISTRIBUTION FUNCTION

In the BET2 code, different options for the initial distribution of the projectile over charge states  $m$  and energy  $E$  are controlled by the parameter `IFEDIST0`. Usually, the initial distribution is normalized to the particle flux equal to unity,

$$H(0) = \sum_m \int f_m(0, E) dE = 1. \quad (9.0.20)$$

Option 1 (`IFEDIST0=1`). An initially mono-charge beam with the ion charge  $MZ = MZ0$  and a box-like energy distribution:

$$f_m(0, E) = \begin{cases} (E_{max} - E_{min})^{-1}, & m = m_0 \wedge E_{min} \leq E \leq E_{max}, \\ 0, & \text{otherwise,} \end{cases} \quad (9.0.21)$$

where the value  $m = m_0$  is determined by the condition  $MZ = MZ0$ .

Option 2 (`IFEDIST0=2`). An initially mono-charge beam with the ion charge  $MZ = MZ0$  and an inverted -parabola energy distribution:

$$f_m(0, E) = \begin{cases} \frac{3}{4 \Delta E} \left[ 1 - \left( \frac{E - E_0}{\Delta E} \right)^2 \right], & m = m_0 \wedge E_0 - \Delta E \leq E \leq E_0 + \Delta E, \\ 0, & \text{otherwise,} \end{cases} \quad (9.0.22)$$

where

$$E_0 = \frac{1}{2}(E_{min} + E_{max}), \quad \Delta E = \frac{1}{\sqrt{2}}(E_{max} - E_{min}), \quad (9.0.23)$$

and the value  $m = m_0$  is determined by the condition  $MZ = MZ_0$ . Here  $E_{max} - E_{min}$  is the full width at half maximum (FWHM) of the initial energy distribution.

In the finite difference scheme, the discrete value  $f_j$  for the interval  $[E_j, E_{j+1}]$  is determined by the condition

$$\int_{E_j}^{E_{j+1}} f(E) dE = \frac{\Delta x_j}{4} (3 - x_j^2 - x_j x_{j+1} - x_{j+1}^2) = f_j (E_{j+1} - E_j), \quad (9.0.24)$$

where

$$x_j = \frac{E_j - E_0}{\Delta E}, \quad \Delta x_j = \frac{E_{j+1} - E_j}{\Delta E}. \quad (9.0.25)$$

Finally we have

$$f_j = \frac{1}{4\Delta E} (3 - x_j^2 - x_j x_{j+1} - x_{j+1}^2). \quad (9.0.26)$$

Option 3 (IFEDIST0=3). An initially mono-charge beam with the ion charge  $MZ = MZ_0$  and a Gaussian energy distribution:

$$f_m(0, E) = \begin{cases} \frac{1}{\sqrt{2\pi}\Omega} \exp\left[-\frac{(E - E_0)^2}{2\Omega^2}\right], & m = m_0 \wedge 0 \leq E \leq \infty, \\ 0, & \text{otherwise,} \end{cases} \quad (9.0.27)$$

where

$$E_0 = \frac{1}{2}(E_{min} + E_{max}), \quad \Omega = \frac{E_{max} - E_{min}}{2\sqrt{2 \ln 2}}, \quad (9.0.28)$$

and the value  $m = m_0$  is determined by the condition  $MZ = MZ_0$ . Here  $E_{max} - E_{min}$  is the full width at half maximum (FWHM) of the initial energy distribution.

In the finite difference scheme, the discrete value  $f_j$  for the interval  $[E_j, E_{j+1}]$  is determined by the condition

$$\int_{E_j}^{E_{j+1}} f(E) dE = f_j (E_{j+1} - E_j), \quad (9.0.29)$$

i.e.

$$f_j = \frac{1}{\sqrt{2\pi}\Omega} \frac{1}{\Delta \xi_j} \int_{\xi_j}^{\xi_{j+1}} e^{-t^2} dt. \quad (9.0.30)$$

where

$$\xi_j = \frac{E_j - E_0}{\Omega\sqrt{2}}, \quad \Delta \xi_j = \xi_{j+1} - \xi_j. \quad (9.0.31)$$

## APPENDIX A: STOPPING THEORY

### A.1. Interpolation between the Bohr and Bethe Coulomb logarithms

The Bohr formula for the Coulomb logarithm (with the relativistic correction due to distant collisions) [1–4] is

$$L_{Br} = \ln \frac{2mv^3\gamma^2}{C|e_1e_2|\bar{\omega}} - \frac{1}{2} \frac{v^2}{c^2}, \quad (A.1.1)$$

where  $e_1$  and  $e_2$  are, respectively, the electric charges of the projectile and field particles,  $m_1$  and  $m_2$  are their masses,  $m = m_1m_2/(m_1 + m_2)$  is the reduced mass,  $v$  is the projectile velocity,  $\ln C = 0.5772156649\dots$  is Euler's constant ( $C = 1.78107241799\dots$ ). The Bohr formula should be applied when

$$\alpha_v = \frac{|e_1e_2|}{\hbar v} \gg 1. \quad (A.1.2)$$

The relativistic Bethe formula [5–7],

$$L_{Bt} = \ln \frac{2mv^2\gamma^2}{\hbar\bar{\omega}} - \frac{v^2}{c^2}, \quad (\text{A.1.3})$$

applies in the opposite limit of  $\alpha_v \ll 1$ . Here we adopt the following simplest interpolation between these two formulae:

$$L = L_{ap} = \ln \frac{2mv^2\gamma^2}{\hbar\bar{\omega}\sqrt{1+C^2\alpha_v^2}} - \frac{v^2}{c^2}. \quad (\text{A.1.4})$$

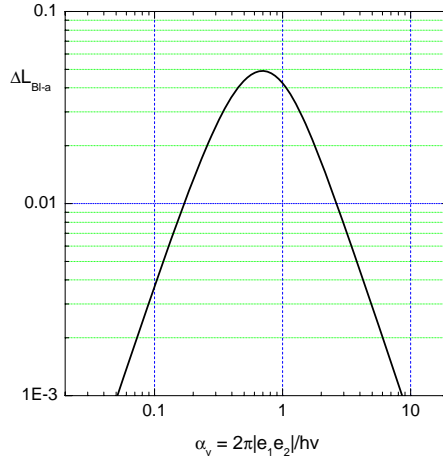


FIG. A.1.1: Accuracy of the interpolation formula (A.1.4) as evaluated by comparing with the Bloch solution.

In our Eq. (A.1.4) the transition between the Bohr and Bethe formulae in the non-relativistic limit (in the relativistic case of  $1 - v^2/c^2 \ll 1$  only the Bethe formula is relevant) is described by the function

$$\phi_{ap}(\alpha_v) = \frac{1}{2} \ln(1 + C^2\alpha_v^2), \quad (\text{A.1.5})$$

where  $L_{ap} = L_{Bt} - \phi_{ap}(\alpha_v)$ . The same transition as calculated by Bloch [8] is described by the function

$$\phi_{Bl}(\alpha_v) = \ln C + \text{Re} \psi(1 + i\alpha_v) = \begin{cases} \alpha_v^2 \left[ \frac{1}{1 + \alpha_v^2} + \frac{1}{2(2^2 + \alpha_v^2)} + \frac{1}{3(3^2 + \alpha_v^2)} + \dots \right], & 0 < \alpha_v < \infty, \\ \ln(C\alpha_v) + \frac{1}{12\alpha_v^2} + \frac{1}{120\alpha_v^4} + \frac{1}{256\alpha_v^6} + \dots, & \alpha_v \gg 1, \end{cases} \quad (\text{A.1.6})$$

where  $L_{Bl} = L_{Bt} - \phi_{Bl}(\alpha_v)$  is the Coulomb logarithm calculated by Bloch. The accuracy of the interpolation (A.1.4) can be evaluated by calculating the difference

$$L_{Bl} - L_{ap} \equiv \Delta L_{Bl-ap} = \Delta L_{Bl-ap}(\alpha_v) = \phi_{ap}(\alpha_v) - \phi_{Bl}(\alpha_v), \quad (\text{A.1.7})$$

which is plotted in Fig. A.1.1. One sees that  $\Delta L_{Bl-ap}$  is always positive and never exceeds 0.05.

## APPENDIX B: MODEL FOR ATOMIC SCREENING

In a partially ionized atom, the remaining bound electrons partially screen the Coulomb potential  $Z/r$  of the nucleus with atomic number  $Z$  (in this section atomic units  $e = \hbar = m_e = 1$  are used). As a result, when a fast electron is scattered off an ion with a net charge  $q$  and  $Z - q$  bound electrons, it “feels” an effective charge  $q_*$ , which is higher than  $q$  and lower than  $Z$ . One of the simplest ways to evaluate  $q_*$  would be to make use of some simple model for unperturbed (static) atomic screening. We expect our screening model to yield a radial dependence  $\eta(r)$  for the net average charge  $\eta$  inside a sphere of radius  $r$  around the nucleus of an ion  $Z^{q+}$ ; evidently,  $\eta(0) = Z$ ,  $\eta(\infty) = q$ . The model described below is constructed as an approximation to the Thomas-Fermi with correct rescaling for H-like ions.

### B.1. The limit of $Z \gg 1$

First of all, we consider a neutral ( $q = 0$ ) atom in the limit of  $Z \rightarrow \infty$ . In this case we would like our model to approach the Thomas-Fermi model of a neutral atom [35], described by the differential equation

$$\frac{d^2\chi}{dx^2} = x^{-1/2} \chi^{3/2}, \quad \chi(0) = 1, \quad \chi(\infty) = 0, \quad (\text{B.1})$$

where the self-similar radial distance  $x$  is defined as

$$x = r b^{-1} Z^{1/3}, \quad b = \frac{1}{2} \left( \frac{3\pi}{4} \right)^{2/3} = 0.885341377. \quad (\text{B.2})$$

In the Thomas-Fermi model, the normalized radial charge distribution is given by

$$\bar{\eta}_{TF0}(x) = Z^{-1} \eta_{TF0}(x) = \chi - x \frac{d\chi}{dx}. \quad (\text{B.3})$$

The charge profile (B.3) is plotted in Fig. B.1 as a dashed curve falling off in proportion to  $x^{-3}$  at  $x \rightarrow \infty$ . It is seen that, although  $d\bar{\eta}_{TF0}(x)/dx|_{x=0} = 0$ , the function  $\bar{\eta}_{TF0}(x)$  can nevertheless at  $x \lesssim 1$  be well approximated by a straight line.

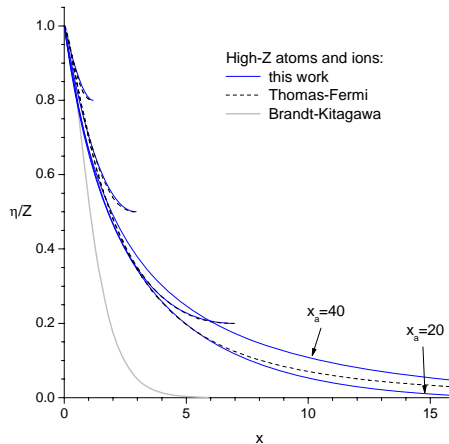


FIG. B.1: Atomic screening: comparison with the Thomas-Fermi model.

For comparison, shown also in Fig. B.1 is the charge profile of the Brandt-Kitagawa [36] model for the case of a neutral atom. In this model, the radial electron density profile has been chosen as  $\propto r^{-1} \exp(-r/r_a)$ , and the screening length (the ion radius)  $r_a = 0.48 Z^{-1/3} (1 - \bar{q})^{2/3} / [1 - (1 - \bar{q})/7]$  was found by minimizing the total energy of the electron cloud. It is clearly seen that the Brandt-Kitagawa charge distribution can hardly be realistic at radial distances  $Z^{-1/3} \lesssim r \lesssim 1-3$  in atoms with  $Z \gg 1$ .

While the Thomas-Fermi charge profile of a neutral atom extends to  $x = \infty$ , all real atoms have finite radii  $r_a \simeq 1-3$ . The latter means that, even for the heaviest of elements with  $Z \approx 90$ , it would make little sense to seek an agreement with the Thomas-Fermi charge distribution at  $x \gtrsim 4-5$ . Hence, we adopt a simple analytical dependence,

$$\bar{\eta}(x) = \frac{(1 - x/x_a)^2}{1 + (0.47 - 2/x_a)x}, \quad 0 \leq x \leq x_a, \quad (\text{B.4})$$

for the normalized charge distribution of a neutral atom, which has the radius  $x_a$  of atom as a free parameter. This dependence has been chosen such as (i) to ensure a vanishing density of bound electrons (proportional to  $x^{-2} d\bar{\eta}(x)/dx$ ) at the atomic boundary  $x = x_a$ , and (ii) to have a fixed slope  $\bar{\eta}(x) = 1 - 0.47x + \dots$  at  $x \ll 1$  independent of the  $x_a$  value. The slope of  $\bar{\eta}(x)$  at  $x = 0$  has been fixed by the condition that at  $x = 1.88$  we recover the Thomas-Fermi value  $\bar{\eta}_{TF0}(1.88) = 0.5$  with  $x_a = 30$ , which is a typical value of  $x_a$  for heavy elements. In other words, our formula (B.4) ensures a reasonable (to an accuracy of about 10%) agreement with the Thomas-Fermi model in the core of the electron cloud (at  $x \lesssim 4$ ) independent of the value  $x_a$  of the atomic radius (within realistic limits), which can be treated as a free parameter. In Fig. B.1 the distribution (B.4) is plotted for two values of  $x_a = 20$  and  $40$ .

By solving the Thomas-Fermi equation (B.1) with the boundary conditions

$$\chi(0) = 1, \quad \chi(x_a) = 0, \quad \bar{\eta}_{TFq}(x_a) = \left( \chi - x \frac{d\chi}{dx} \right)_{x=x_a} = \bar{q} \equiv \frac{q}{Z}, \quad (\text{B.5})$$

one can calculate the finite radius  $x_a$  and the charge distribution  $\bar{\eta}_{TFq}(x)$  of an isolated ion with the normalized ionization degree  $\bar{q}$  [35] in the limit of  $Z \gg 1$ . Figure B.1 shows the three corresponding curves for  $\bar{q} = 0.2, 0.5$  and  $0.8$ . It is clearly seen that for different  $q$  values the profiles  $\bar{\eta}_{TFq}(x)$  all rapidly approach the same curve  $\bar{\eta}_{TF0}(x)$  as  $x \rightarrow 1$ . The latter is a natural consequence of the fact that the first term of expansion of  $\bar{\eta}_{TFq}(x) = 1 - \frac{2}{3}x^{3/2} + \dots$  does not depend on  $q$ .

Now, we generalize our approximate expression (B.4) for the neutral atom to an arbitrary ion by writing

$$\bar{\eta}(x) = \begin{cases} \bar{q} + (1 - \bar{q}) \frac{(1 - x/x_a)^2}{1 + [0.47(1 - \bar{q})^{-2/3} - 2/x_a]x}, & 0 \leq x \leq x_a, \\ \bar{q}, & x_a \leq x. \end{cases} \quad (\text{B.6})$$

To have an invariant slope of  $\bar{\eta}(x)$  at  $x \ll 1$ , we must have put  $0.47(1 - \bar{q})^{-1}$  instead of  $0.47(1 - \bar{q})^{-2/3}$  in the denominator of Eq. (B.6), but this would have led to incorrect scaling for hydrogen-like ions (see below). The difference between these two cases becomes noticeable only at  $1 - \bar{q} \ll 1$ , when the Thomas-Fermi model breaks down anyway. In Fig. B.1 our approximate profile Eq. (B.6) is compared with the Thomas-Fermi profiles (at  $x \leq x_a$ , where the  $x_a$  values are taken from the Thomas-Fermi solution) for three values of  $\bar{q} = 0.2, 0.5$  and  $0.8$ . In all cases a good agreement is observed.

When transformed back to the normal radial coordinate  $r = bZ^{-1/3}x$  (in atomic units), Eq. (B.6) becomes

$$\eta(r) = \begin{cases} q + (Z - q) \frac{(1 - r/r_a)^2}{1 + [0.53 Z(Z - q)^{-2/3} - 2/r_a] r}, & 0 \leq r \leq r_a, \\ q, & r_a \leq r. \end{cases} \quad (\text{B.7})$$

### B.2. Hydrogen atom and hydrogen-like ions

For the hydrogen atom Eq. (B.7) yields

$$\eta_H(r) = \frac{(1 - r/r_H)^2}{1 + (0.53 - 2/r_H)r}, \quad 0 \leq r \leq r_H. \quad (\text{B.8})$$

This function is plotted in Fig. B.2 for two values of  $r_a = r_H = 5$  and  $3$ , and compared with the exact charge distribution,

$$\eta_{1s}(r) = (1 + 2r + 2r^2) e^{-2r}, \quad (\text{B.9})$$

for the hydrogen atom in the  $1s$  ground state [35]. One sees that a reasonable agreement (to the extent that can be expected from a Thomas-Fermi based approach for  $Z = 1$ ) is achieved for  $r_a = 5$ . The charge distribution  $\eta_H(r)$  in the hydrogen atom is obviously rescaled to any H-like ion,  $\eta_{Z-1}(r) = Z - 1 + \eta_H(rZ)$ ,  $r < r_H/Z$ . One readily verifies that Eq. (B.7) obeys this scaling law.

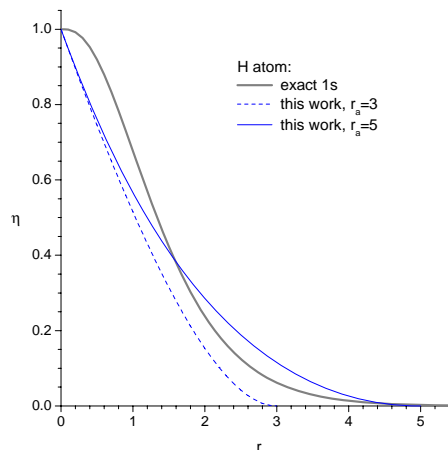


FIG. B.2: Atomic screening of the hydrogen atom.

### B.3. Ionic radius $r_a$

To obtain a realistic estimate of the radius  $r_a$  for an arbitrary ion  $Z^{q+}$ , we assume that the ionization potential  $I_q$  (in atomic units) of this ion is known (either from experiment or atomic calculations). Then, knowing the  $r_a$  value for the hydrogen atom, we can rescale it to an arbitrary ion as

$$r_a = 2.5 \frac{1 + q}{I_q}. \quad (\text{B.10})$$

Such a rescaling is based on a simplifying assumption that the outer electron, whose binding energy is  $I_q$ , moves in the Coulomb field of a point charge  $q + 1$ ; then, by virtue of the virial theorem, we must have  $I_q \propto (1 + q)/r_a$ . Since for the H-like ions  $I_{Z-1} = \frac{1}{2}Z^2$ , Eq. (B.10) yields  $r_a = 5/Z$  for these ions.

Clearly, for our approximation (B.7) to be meaningful, the denominator on its right-hand side should be positive for all  $0 < r \leq r_a$ . With  $r_a$  given by Eq. (B.10), the closest approach to this situation occurs for the He atom, for which  $r_a = 2.77$ , and the denominator in Eq. (B.7) becomes  $1 - 0.055r$ ; but even in this case we are still far from the unwanted singularity.

#### B.4. Momentum transfer to a fast electron

When a fast electron with a velocity  $v$  passes by an atom with a charge distribution (B.7) at an impact parameter  $b$ , its trajectory can be approximated as a straight line, and the classical momentum transfer  $|\Delta p|$  (in atomic units) can be calculated as

$$|\Delta p| = \frac{2b}{v} \int_0^\infty \frac{\eta(\sqrt{b^2 + s^2})}{(b^2 + s^2)^{3/2}} ds = \frac{2}{vb} \int_0^{\pi/2} \eta\left(\frac{b}{\cos\theta}\right) \cos\theta d\theta. \quad (\text{B.11})$$

The straight-line approximation is justified for  $|\Delta p| \ll v$ , i.e. for  $v^2 \gg 2\eta(b)/b$ . The integration on the right-hand side of Eq. (B.11) can be carried out analytically, with the result given by

$$\int_0^{\pi/2} \eta\left(\frac{b}{\cos\theta}\right) \cos\theta d\theta = \begin{cases} q + (Z - q) \left[ \sqrt{1 - \bar{b}^2} - \bar{b}(\alpha + 2) \arcsin \sqrt{1 - \bar{b}^2 + \bar{b}^2(\alpha + 1)^2} \phi \right], & 0 < b < r_a, \\ q, & r_a \leq b, \end{cases} \quad (\text{B.12})$$

where

$$\phi = \phi(\alpha, \bar{b}) = \begin{cases} \frac{1}{\sqrt{1 - \alpha^2 \bar{b}^2}} \ln \frac{1 + \alpha \bar{b} + \sqrt{1 - \alpha^2 \bar{b}^2} \sqrt{(1 - \bar{b})/(1 + \bar{b})}}{1 + \alpha \bar{b} - \sqrt{1 - \alpha^2 \bar{b}^2} \sqrt{(1 - \bar{b})/(1 + \bar{b})}}, & 0 < \alpha \bar{b} < 1, \\ \frac{2}{\sqrt{\alpha^2 \bar{b}^2 - 1}} \arctan \sqrt{\frac{(\alpha \bar{b} - 1)(1 - \bar{b})}{(\alpha \bar{b} + 1)(1 + \bar{b})}}, & 1 < \alpha \bar{b}, \end{cases} \quad (\text{B.13})$$

and

$$\alpha = 0.53 \frac{r_a Z}{(Z - q)^{2/3}} - 2, \quad \bar{b} = \frac{b}{r_a}. \quad (\text{B.14})$$

- 
- [1] N. Bohr, *Philos. Mag.* **25** (1913) 10.  
[2] N. Bohr, *Philos. Mag.* **30** (1915) 581.  
[3] J. D. Jackson, *Classical Electrodynamics*, 2nd edition (Wiley, New York, 1975), Chap. 13.  
[4] S. P. Ahlen, *Rev. Mod. Phys.* **52** (1980) 121.  
[5] H. Bethe, *Ann. Physik* **5** (1930) 325.  
[6] H. Bethe, *Z. Physik* **76** (1932) 293.  
[7] C. Møller, *Ann. Physik* **14** (1932) 531.  
[8] F. Bloch, *Ann. Phys. (Leipzig)* **16** (1933) 285.  
[9] E. Fermi and E. Teller, *Phys. Rev.* **72** (1947) 399.  
[10] R. H. Ritchie,  
[11] T. Hamada, *Aust. J. Phys.* **31** (1978) 291.  
[12] M. M. Basko, *Eur. Phys. J. D* **00** (2004) 000.  
[13] M. M. Basko, *Fiz. Plazmy* **10** (1984) 1195 (English translation: *Sov. J. Plasma Phys.* **10** (1984) 689).  
[14] Lotz, *Z. Physik* **216** (1968) 241.  
[15] Lotz, *Z. Physik* **220** (1969) 466.  
[16] I.D.Kaganovich, E.A.Startsev, and R.C.Davidson, *Phys. Plasmas* **11** (2004) 1229.  
[17] J.J.Thomson, *Philos. Mag.* **23** (1912) 449.  
[18] R.K.Janev, L.P.Presnyakov, and V.P.Shevelko, *Physics of Highly Charged Ions* (Springer, Berlin, 1985).  
[19] S.Y.Ovchinnikov, *Phys. Rev. A* **42** (1990) 3865.  
[20] I.D.Kaganovich, E.A.Startsev, and R.C.Davidson, Report PPPL-3819 (2004), Princeton Plasma Physics Laboratory, Princeton University; <http://www.osti.gov/dublinkcore/gps/purl/814022-BYDtRM/native/>.  
[21] E.J.McGuire, *Phys. Rev. A* **22** (1980) 868.  
[22] M.E. Rudd, Y.-K. Kim, D.H.Madison, J.W. Callagher, *Rev. Mod. Phys.* **57** (1985) 965.  
[23] Atomic Data for Fusion. Volume 1: Collisions of H, H<sub>2</sub>, He and Li Atoms and Ions with Atoms and Molecules (Ed. C. F. Barnett) ORNL-6086 (1990); <http://www-cfadc.phy.ornl.gov/redbooks/>.  
[24] M. B. Shah, P. Mc. Callion, and H. B. Gilbody, *J. Phys. B* **22** (1989) 3037.  
[25] N. Bohr, *K. Dan. Vidensk. Selsk. Mat. Fys. Medd.* **18**, 8 (1948).  
[26] H. Tawara and A. Russek, *Rev. Mod. Phys.* **45** (1973) 178.  
[27] M. B. Shah, D. S. Elliott, and H. B. Gilbody, *J. Phys. B* **20** (1987) 2481.  
[28] P. M. Stier, C. F. Barnett, *Phys. Rev.* **103** (1956) 896.  
[29] L. M. Brown, *Phys. Rev.* **79** (1950) 297.  
[30] M.C. Walske, *Phys. Rev.* **88** (1952) 1283.  
[31] L.H. Toburen, M.Y. Nakai, R.A. Langley, *Phys. Rev.* **171** (1968) 114.  
[32] R.A. Phaneuf, R.K. Janev, and H.T. Hunter, *Nucl. Fusion (Special Suppl. 1987)* (1987) 7.

- [33] H. Knudsen, H.K. Haugen, and P. Hvelplund, Phys. Rev. A **24** (1981) 2287.
- [34] F.W. Meyer, R.A. Phaneuf, H.J. Kim, P. Hvelplund, and P.H. Stelson, Phys. Rev. A **19** (1979) 515.
- [35] L. D. Landau and E. M. Lifshitz, *Quantum Mechanics* (...), 1989).
- [36] W. Brandt and M. Kitagawa, Phys. Rev. B **25** (1982) 5631.
- [37] Ya.B. Zel'dovich, Yu.P. Raizer, *Physics of Shock Waves and High-Temperature Hydrodynamic Phenomena*, (Academic Press, New York and London, 1966-67).
- [38] V.P. Shevelko, Z. Physik A **287** (1978) 19.
- [39] L.A. Vainshtein, I.I. Sobel'man, and E.A. Yukov, *Vozbuzhdenie atomov i ushirenie spektral'nyh linii*, ("Nauka", Moscow, 1979).